DEPARTMENT OF THE NAVY
BUREAU OF WEAPONS
Contract NOrd 18594

Final Report

Technical Report No. 6

THERMO-VISCOELASTIC STRESSES IN A SPHERE WITH AN ABLATING CAVITY

by

T. G. Rogers and E. H. Lee

Brown University

DIVISION OF APPLIED MATHEMATICS
BROWN UNIVERSITY
PROVIDENCE, R.I.

August 1962

NORD-18594/6

Nord-18594-Final Report

Thermo-viscoelastic Stresses in a Sphere with an Ablating Cavity*.

T. G. Rogers and E. H. Lee
Brown University

Abstract

Thermo-viscoelastic stresses in a sphere with a concentric spherical cavity are analysed, for uniform initial temperature, and cavity ablation at an elevated constant surface temperature. The material is considered to be thermo-rheologically simple, with properties prescribed by an isothermal relaxation modulus function and a relaxation time scale factor given as a function of the temperature. The theory is developed in the form of integral equations in time for the radial stress gradient. These lend themselves to numerical solution, and an example is presented of a sphere of polymethyl-methacrylate for which the relaxation modulus function and temperature-log(time) shift function are available. Features of the solution are discussed, and compared with a corresponding elastic case and the previously published solution for an ablating solid sphere.

* This work was sponsored by the Bureau of Weapons, Department of the Navy, under Contract NOrd 18594 with Brown University.

Introduction

This paper is concerned with thermal stresses in a linear viscoelastic material in which increase in temperature produces thermal expansion with coefficient α, and also contracts the time scale of the relaxation modulus (and creep compliance) by a factor $\varphi(T)$, where T is the temperature measured above a base temperature T_o. The response to stress at different temperatures of many materials can be expressed by relations of this type [1]*, termed thermo-rheologically simple behavior by Schwarzl and Staverman [2], and known in the chemical literature as the Williams-Landel-Ferry law. On the common log(time) plot, this corresponds to change in temperature causing a shift of the relaxation curve along the log(time) axis without change of shape.

In order to deal with varying (time-dependent) temperature, with the resulting contraction of the time scale thus itself a function of time, it is convenient [3] to define a reduced time ξ which incorporates the varying scale factor $\varphi(T)$, so that in terms of ξ the viscoelastic stress-strain relation at varying temperature has the same form as the isothermal law at the base temperature T_o:

$$s_{ij}(x,\xi) = \int_0^{\xi} 2G(\xi-\xi') \frac{\partial e_{ij}(x,\xi')}{\partial \xi'} d\xi' , \qquad (1)$$

where x denotes the triplet of rectangular Cartesian coordinates

* Numbers in square brackets refer to the bibliography at the end of the paper.

(x_1,x_2,x_3), s_{ij} and e_{ij} are the stress and strain deviators respectively, and $G(t)$ is the relaxation modulus in shear at the base temperature T_o*. The reduced time $\xi(x,t)$, where t is the real time, is determined in terms of the varying scale factor $\varphi[T(x,t)]$ by the relation

$$\xi(x,t) = \int_0^t \varphi[T(x,t')]dt'. \qquad (2)$$

During the course of the analysis we shall find it convenient to consider a dependent variable, for example the stress deviator, sometimes to be a function of the reduced time ξ: $s_{ij}(x,\xi)$, and sometimes expressed in terms of the real time, and we shall use the same function notation: $s_{ij}(x,t)$. This signifies replacing ξ in $s_{ij}(x,\xi)$ by $\xi(x,t)$. The functional form is thus different, but no confusion need arise since the independent variables will either be stated or be clear from the context. Space derivatives, e.g. $\frac{\partial s_{ij}}{\partial x_j}$, will always signify differentiation at constant real time t, since they will arise only from the equilibrium and displacement-strain relations, which involve space gradients at fixed real time. Since a transformation from t to ξ may be involved in, for example, the interpretation of an integral over reduced time of a space derivative, a distinguishing function notation would become cumbersome in the present problem.

The integral operator form of the viscoelastic stress-strain relation (1) is utilized because of its generality

---

* Only the relationship (1) for shear type deformation has been stated since we shall assume the response in dilatation to be elastic.

compared with the low-order differential operator laws commonly considered in viscoelastic stress analysis solutions. This generality permits accurate representation of material response over the equivalent of a wide frequence band, and is needed in thermal-stress problems because of the sensitivity of the scale factor φ to temperature change. Moreover, the integral operator law can lead to representation of the stress distribution sought as the solution of an integral equation with its kernel dependent on the relaxation modulus $G(t)$. Numerical solution by finite sum methods may prove convenient [4], and permits direct substitution of the experimentally measured material characteristics into the analysis.

In this paper we treat the problem of a sphere with a concentric spherical cavity. The temperature is initially uniform throughout, when that at the cavity surface increases discontinuously to a value which is thereafter maintained constant, and the cavity ablates with steadily increasing radius until it reaches the outer radius, and the viscoelastic material has then disappeared. Such a problem falls within the general framework of the method devised by Muki and Sternberg [5], but the moving boundary rules out application of the Laplace transform, and integral operator expressions must be maintained to yield integral equation formulations which can cope with the moving boundary [4]. This aspect of the analysis was developed in [6], but it was applied there only to the problem of a solid sphere in which the coupling between the elemental spherical

shells happens effectively to disappear because of symmetry requirements at the center. In the present problem the spherical shell solutions are linked by the stress boundary conditions at the surfaces, and this leads to coupling in the space variables of the integral equations in time, and so to a much more challenging computational task. This coupling, incidentally, rules out the transform approach even for fixed boundaries, since the resulting integral equation is, in general, no longer of convolution type, as pointed out by Sternberg and Gurtin [7].

The spherically symmetric stress field.

A body in the form of a spherical shell is considered, loaded uniformly over each surface and subjected to a radially symmetrical temperature distribution $T(r,t)$, where r is the radius. A brief development of the theory given in [6] is presented here to provide a framework for discussion of the new solution. Symmetry determines the principal stresses to be the radial stress σ_r and the circumferential stress σ_θ repeated. The sum of the principal stresses is therefore:

$$\sigma = \sigma_r + 2\sigma_\theta. \tag{3}$$

The single non-trivially satisfied equilibrium equation in

$$\frac{\partial \sigma_r}{\partial r} + \frac{2}{r}(\sigma_r - \sigma_\theta) = 0. \tag{4}$$

Symmetry determines a single independent stress deviator component, and a corresponding strain deviator component, which for convenience can be replaced by principal stress and strain

differences. With $u(r,t)$ as the radial displacement, the equivalent of (1) then becomes

$$\sigma_\theta(r,\xi) - \sigma_r(r,\xi) = \int_0^\xi 2G(\xi-\xi') \frac{\partial}{\partial \xi'} [\frac{u}{r} - \frac{\partial u}{\partial r}] d\xi' \qquad (5)$$

which, using (4), can be written in the form

$$\frac{\partial \sigma_r}{\partial r} = - \int_0^\xi 4G(\xi-\xi') \frac{\partial}{\partial \xi'} [\frac{\partial}{\partial r}(\frac{u}{r})] d\xi' \ . \qquad (6)$$

Note that, as mentioned in the Introduction, the r derivatives operate on functions of r and t, but transformation to r and ξ is implied for the integration. σ_θ can be eliminated from (3) and (4) to give:

$$\frac{\partial}{\partial r} (r^3 \sigma_r) = r^2 \sigma \ . \qquad (7)$$

Elastic dilatational response is assumed, together with thermal expansion with constant coefficient α, giving the relation

$$\sigma = 3k[\frac{\partial u}{\partial r} + \frac{2u}{r} - 3\alpha\Theta], \qquad (8)$$

where k is the bulk modulus and Θ the increase in temperature over the uniform initial temperature. Integration of (7) at constant real time and substitution for σ from (8) yields

$$r^3\sigma_r(r,t) - [a(t)]^3\sigma_r[a(t),t] = 3k[r^2u(r,t) - [a(t)]^2u[a(t),t] - 3\alpha \int_{a(t)}^{r} \rho^2\Theta(\rho,t)d\rho] \ , \qquad (9)$$

in which conditions at a boundary radius a(t) give the lower limits of the integrals. Substitution for u(r,t) from (9) into (6) gives:

$$\frac{\partial \sigma_r}{\partial r} = -4 \int_0^{\xi} G(\xi-\xi') \frac{\partial}{\partial \xi'}\left[\frac{1}{3k}\frac{\partial \sigma_r}{\partial r} + \frac{3a^3}{r^4}\left\{\frac{\sigma_r(a,t')}{3k} - \frac{u(a,t')}{a}\right\}\right.$$

$$\left. + \frac{3\alpha}{r^4}\left\{\int_a^r \rho^3 \frac{\partial \Theta}{\partial \rho}\, d\rho + a^3\Theta(a)\right\}\right] d\xi' \qquad (10)$$

The ξ' integral is a convolution integral (see, for example, Tricomi [8]), and this provides a simplification of (10) through the associative property of convolutions. We define the function $R(\xi)$ by the integral equation

$$R(\xi) + \frac{4}{3k}\int_0^{\xi} G(\xi-\xi') \frac{\partial R(\xi')}{\partial \xi'}\, d\xi' = 2G(\xi) \qquad (11)$$

which, it will be noted, contains the same operator on R as does (10) on $\frac{\partial \sigma_r}{\partial r}$. The associative property of convolutions then enables (10) to be replaced by:

$$\frac{\partial \sigma_r}{\partial r} = \int_0^{\xi} R(\xi-\xi')\frac{\partial}{\partial \xi'}\left[-\frac{6a^3}{r^4}\left\{\frac{\sigma_r(a,t')}{3k} - \frac{u(a,t')}{a}\right\}\right.$$

$$\left. - \frac{6\alpha}{r^4}\left\{\int_a^r \rho^3 \frac{\partial \Theta}{\partial \rho}\, d\rho + a^3\Theta(a)\right\}\right]. \qquad (12)$$

We consider an ablating hollow sphere, and take a(t) to be the varying cavity radius. The surface boundary conditions are then:

$$r = a(t),\ \sigma_r[a(t),t] = f_1(t);\ r = b(t),\ \sigma_r[b(t),t] = f_2(t) \qquad (13)$$

where b(t) is the radius of the external surface, and $-f_1(t)$, $-f_2(t)$ are prescribed surface pressures. Since u(a,t) is not known a priori, the integrand in (12) contains an unknown function of t, and it is convenient to combine this with other functions of t only and write (12) in the form

$$\frac{\partial \sigma_r}{\partial r} = -\frac{6\alpha}{r^4}\int_0^{\xi} R(\xi-\xi')\frac{\partial}{\partial \xi'}\left[f(t') + \int_{a(t')}^{r} \rho^3 \frac{\partial \Theta}{\partial \rho}\, d\rho\right] d\xi' , \qquad (14)$$

where

$$f(t) = -\frac{[a(t)]^3}{\alpha}\left\{-\frac{\sigma_r[a(t),t]}{3k} + \frac{u[a(t),t]}{a(t)} - \alpha\Theta[a(t),t]\right\} . \qquad (15)$$

Integration of (14) through the sphere at constant real time, using the boundary conditions (13) to give:

$$\int_{a(t)}^{b(t)} \frac{\partial \sigma_r}{\partial \rho}\, d\rho = f_2(t) - f_1(t) \qquad (16)$$

reduces (14) to an integral equation for f(t). Because ξ is a function of r and t, this space integral destroys the simplifying convolution property of the integral equation over reduced time, but, as shown below, it can be readily solved numerically by finite sum techniques. f(t) having been determined, (12) comprises an integral for $\frac{\partial \sigma_r}{\partial r}$, space integration from a boundary gives σ_r, and σ_θ is then determined from (4).

Method of solution.

Since the functions which define the problem -- the temperature field $\Theta(r,t)$, the boundary radii a(t) and b(t) and the prescribed pressures $-f_1(t)$, $-f_2(t)$ -- are all defined in terms of real time t, and since the benefit to be gained by using ξ as independent variable has already been achieved through the application of convolution theory leading to (12), it is advantageous to evaluate the solution in terms of the real time t. Equation (14) then becomes

$$\frac{\partial \sigma_r}{\partial r} = -\frac{6\alpha}{r^4}\int_0^t R[\xi(r,t)-\xi(r,t')]\frac{\partial}{\partial t'}[f(t') + \int_{a(t')}^{r} \rho^3 \frac{\partial \Theta}{\partial \rho}\, d\rho]dt'. \quad (17)$$

Integrating by parts to obtain a more convenient form for numerical integration yields the expression

$$\frac{\partial \sigma_r}{\partial r} = -\frac{6\alpha}{r^4}[R(0)\{f(t) + \int_{a(t)}^{r} \rho^3 \frac{\partial \Theta}{\partial \rho}\, d\rho\}$$

$$- \int_0^t \{f(t') + \int_{a(t')}^{r} \rho^3 \frac{\partial \Theta}{\partial \rho}\, d\rho\} \frac{\partial}{\partial t'} R\{\xi(r,t)-\xi(r,t')\}dt'].$$

(18)

As described in [4], a suitable finite sum approximation for the time integral in (18) is obtained by placing ahead of the integral sign a mean value of the first bracket of the integrand. Equation (18) can then be written in the form

$$-r^4 \frac{\partial \sigma_r}{\partial r} = R_n[f(t_n) + h(r,t_n)]$$

$$- \frac{1}{2}\sum_{k=1}^{n-1} [f(t_k) + h(r,t_k) + f(t_{k+1}) + h(r,t_{k+1})][R_{k+1}-R_k]$$

(19)

where

$$R_k = R[\xi(r,t_n) - \xi(r,t_k)] \quad (20)$$

$$h(r,t_k) = \int_{a(t_k)}^{r} \rho^3 \frac{\partial \Theta(\rho,t_k)}{\partial \rho}\, d\rho \quad (21)$$

and, in order to remove the constant 6α, the functions have been normalized with the new σ_r given by $\sigma_r/6\alpha E\Theta_1$, where E is the instantaneous Young's modulus, and Θ_1 the maximum temperature difference occurring.

By integrating the finite sum equation (19) over the radius, $f(t_n)$ is given in terms of its value at earlier times; hence the terms containing $f(t_n)$ are grouped together, and (19) is written in the form

$$2\frac{\partial \sigma_r}{\partial r} = P + \frac{R_n f(t_{n-1})}{r^4} - f(t_n)(D + \frac{R_n}{r^4}) \tag{22}$$

where

$$r^4 P = [h(r,t_{n-1}) + h(r,t_n) + f(t_{n-1})][R_n - R_{n-1}]$$

$$- [2h(r,t_n) + f(t_{n-1})R_n]$$

$$+ \sum_{k=1}^{n-2} [h(r,t_k) + h(r,t_{k+1}) + f(t_k) + f(t_{k+1})][R_{k+1} - R_k]$$

and

$$r^4 D = R_{n-1} .$$

We consider the case with zero surface pressure so that $f_1(t) \equiv f_2(t) \equiv 0$, and constant external radius $b(t) \equiv b$. Integration of (22) over r from a(t) to b then yields

$$0 = \int_{a(t)}^{b} P dr + f(t_{n-1})G - f(t_n)[\int_{a(t)}^{b} D dr + G] \tag{23}$$

where

$$G = \frac{R_n}{3}\{[a(t_n)]^{-3} - b^{-3}\} .$$

Equation (23) determines $f(t_n)$ in the form

$$f(t_n) = \frac{\int_{a(t)}^{b} P dr + f_{n-1} G}{\int_{a(t)}^{b} D dr + G} \tag{24}$$

with the solution immediately after application of the surface temperature, at $t=0^+$, defining $f(0) = 1$. Substitution of $f(t_n)$ into (22) and integration from the fixed outside boundary r=b determines σ_r according to

$$2\sigma_r(r,t_n) = \frac{R_n}{3}[f(t_n) - f(t_{n-1})][r^{-3}-b^{-3}] - \int_r^b P\,dr + f(t_n)\int_r^b D\,dr. \tag{25}$$

The integrals over r were evaluated by using Simpson's rule over most of the range, but the trapezoidal rule for a single step only and the Newton-Cotes three interval expression adjacent to the boundary r=b for odd numbers of intervals greater than one. Next to the moving boundary, r=a(t), it was necessary to use unequal steps in r, and the finite sum integration formula was chosen to give the area under a parabola through the last three points. The choice of interval size for both n and t is discussed in the next section where the solution is presented. The calculations were carried out on the IBM-7070 machine at the Brown University Computing Laboratory.

The temperature variation $\Theta(r,t)$ was obtained as the solution of the heat conduction problem, neglecting the coupling between heat energy and mechanical energy dissipated in viscoelastic flow. For the thermal stress problem mentioned in the Introduction, we need the temperature field in a sphere initially at uniform temperature, defined as zero, and with the constant temperature Θ_1 at the ablating surface. To limit computational effort on this particular problem, which is evaluated simply as

an example of a class of solutions, a temperature field given by a relatively simple expression was achieved by considering the cavity to be in an infinite medium and by making use of the analogy between plane and spherically symmetric heat flow mentioned in [9]. The resulting solution involves heat conduction across the radius r=b, which determines the outer boundary condition for the temperature distribution in the spherical shell. We consider the temperature field for $r \geq a(0) = a$, when the variation

$$\frac{\Theta}{\Theta_1} = 1 + \frac{\beta}{\sqrt{\pi}} t^{\frac{1}{2}} + \gamma t + \frac{\delta}{4} t^2 \qquad (26)$$

is prescribed on the surface r=a, where β, γ and δ are arbitrary constants. The locus r=a(t) determined by $\Theta=\Theta_1$ can be considered as the ablating boundary, which can be located from the known temperature distribution corresponding to the boundary condition (26) at r=a, and zero initial temperature (see [9])

$$\frac{\Theta}{\Theta_1} = \frac{a}{r}[\operatorname{erfc} x + \beta t^{\frac{1}{2}} \operatorname{ierfc} x + \gamma t(4\, i^2\operatorname{erfc} x) + \delta t^2(8\, i^4\operatorname{erfc} x)] \qquad (27)$$

where $x = (r-a)/2(Kt)^{\frac{1}{2}}$, K being the thermal diffusivity. The second term with $\beta \neq 0$ is needed to ensure finite initial velocity for the ablating boundary, and the constants were chosen to achieve approximately constant rate of ablation. Figure 1 shows the resulting curve, r=a(t), for $\alpha = 2.871$, $\beta=2$ and $\gamma=2000$, compared with that for constant velocity ablation. For the

numerical solution the positions of the ablating boundary, $r=a(t_k)$, were determined by solving (27) for x by Newton's method, with the left hand side replaced by unity. Equation (27) then determines the temperature field for $a(t_k) \leq r \leq b$, and the resulting distributions are shown in Fig. 2 at four time values. As seen from Fig. 1, the average velocity of ablation was selected to complete the process, $a(t)=b$, at $t = 0.7a^2/K$, for the outside boundary chosen, $b=3a$. Immediately after application of the internal heat, at $t=0^+$, the cavity surface is at temperature Θ_1, with the rest of the material still at the zero initial temperature. The temperature field does not correspond to one of the standard boundary conditions for heat conduction, but a glance at the distributions adjacent to $r=3a$ suggests that the temperature gradient is roughly proportional to the temperature, so that the solution approximates the radiation condition $\frac{d\Theta}{dr} = -H\Theta$. From (27) the integrals (21) for $h(r,t_k)$ can readily be evaluated.

As in the problem discussed in [6], the thermal stress field was evaluated for polymethyl-methacrylate material behavior using measured tensile relaxation data. We use the auxiliary function $R(\xi)$ evaluated in [4] by numerical integration of an integral equation equivalent to (11). The shift function $\varphi(T)$ used by Muki and Sternberg [5] was used, and also the same temperature range, $\Theta_1 = 30^\circ C$ with the initial temperature $80^\circ C$. Taking $K = 8$ cms^2/hr, and $a = 4$ cms, the total time of ablation becomes $0.7\ a^2/K = 1.4$ hrs. As discussed in [6], formally the

solution applies for a range of a and K, with constant a^2/χ, but since viscoelastic characteristics for polymethyl-methacrylate have been used, for practical interpretation the corresponding value of K must also be substituted.

The solution

Using the material data and constants defining the particular problem to be solved, time and space steps for the finite sum integration procedures detailed in the previous section were determined by trial. Increments were halved until inappreciable differences in the solution resulted. The full line in Fig. 3 shows the variation of f(t) defined in (15), with $\sigma_r[a(t),t] = 0$ for the case considered of zero cavity pressure. It will be noted that, apart from the factor $-[a(t)]^3$, f(t) then represents the excess of the circumferential strain at the cavity surface over the thermal expansion there, and is thus the strain caused by stress. It was computed according to (24). As detailed in the previous section, f(t) is the function which links the stress values at different radii, and constitutes a major ingredient of the stress determination. It must therefore be determined accurately, and the choice of time and space steps was assessed by their influence on f(t). The results shown in Fig. 3 were calculated for $\Delta r/a = 0.05$, and for the early stages $K\Delta t/a^2 = 0.0125$. The availability of memory locations limited the time range over which this fine time mesh could be maintained, but increasing the step for intermediate times caused no difficulty

since temperature gradients, and the resulting dependent variables, settle down to more gradual variation. When ablation is almost complete, and only a thin shell of material remains, f(t) changes rapidly and accuracy again demands a reduction in the time step. With only a narrow shell left, smaller increments in the radius would also be needed to maintain accuracy, and the completion of the f(t) curve up to $Kt/a^2 = 0.7$ was achieved by an analytical expansion procedure. That the finite increments stated above are small enough for satisfactory accuracy is indicated by the comparisons of f(t) values computed for different finite difference steps presented in Table I. With a radius step of $\Delta r/a=0.1$ an undesirable roughness was apparent in the f(t) values due to the change in the form of the space integrals in (21) and (24) as the number of radius increments spanning the ablating shell changed from odd to even, and as the size of the interval adjacent to the ablating boundary changed. This roughness was not apparent for $\Delta r/a = .05$.

The individual points plotted in Fig. 3 correspond to the solution for an elastic body with the elastic constants for instantaneous loading of polymethyl-methacrylate. It is obtained by simply substituting $R(\xi) = R(0)$, a constant, into the viscoelastic analysis.

Computed values of σ_r and σ_θ, evaluated from (25) and (4) are plotted in Figs. 4 to 7 for both the viscoelastic and elastic cases. Use of the time and space steps found satisfactory for determining f(t)lead to satisfactory accuracy over most of

the radius range, but to serious inaccuracies adjacent to the ablating boundary in the viscoelastic case. These occur because the temperature rise at the ablating surface results in accelerated stress relaxation due to the sensitivity of the scale factor $\varphi(T)$ to temperature. Taking the initial temperature as the base temperature, φ is $10^{3.6}$ at the ablating surface, so that relaxation times are all reduced by this factor with the resulting rapid stress relaxation shown. In order to improve accuracy in the region of the ablating boundary, integration of (22) for σ_r was carried out from the inner boundary a(t) using time steps of .00125 a^2/K, and space steps of $\Delta r/a = .0125$. Corresponding values of f(t) were deduced by interpolation. Results of these calculations are shown by the circled points in Fig. 4, and they are seen to veer smoothly into the values calculated for the larger mesh away from the inner boundary. Points corresponding to the latter are indicated by crosses and are seen to be appreciably in error near the boundary. Similar corrections were needed at later values of the time, though somewhat larger time steps could be tolerated, and were necessitated by machine storage limitations, unless more elaborate programming techniques were to be utilized. As mentioned above, smaller time and radius steps were needed to maintain accuracy near the end of the process when only a thin spherical shell remained, and these could be incorporated since only a small radius range occurred.

Study of the results depicted in Figs. 3 to 7 reveal interesting features of the solutions. The stress distributions show that the influence of viscoelasticity is large but localized in the heated region near the ablating boundary, in conformity with the sharp influence of temperature on viscoelasticity through the scale factor $\varphi(T)$. The main body of the material thus responds essentially elastically. The thermal expansion near the ablating surface is resisted by the constraint of these outer layers, and this leads to the high peak of circumferential compression. Immediately on application of the cavity surface temperature Θ_1, at $t=0^+$, the strain is completely constrained to remain zero, and the cavity surface is subjected to a surface compression of magnitude 0.2564, as discussed in [6] for the solid sphere. Qualitatively, constraint of this nature remains until ablation is almost complete as indicated by the variation of $f(t)$, which, as mentioned above, is a function of the circumferential expansion at the cavity surface due to stress alone. For quantitative assessment, the factor $-[a(t)]^3$ must be taken into account. The rapid decrease in $f(t)$ shown in Fig. 3 when ablation is nearly complete represents freedom for thermal expansion when the temperature rise spreads to the outer boundary, and a consequent decrease in magnitude of the negative strain due to the compressive stress. In the elastic case the strain just prior to complete ablation is entirely due to thermal expansion, since stresses reduce to zero with no surface pressure acting, and hence $f(t_b) = 0$, where $a(t_b) = b$. For the viscoelastic case,

the outer ring has been stressed in tension throughout the process, and so a positive residual strain due to viscoelastic flow is superposed on the thermal strain, and $f(t_b)$ becomes negative as shown.

An indication of the effectiveness of the constraint of the outer part of the sphere is provided by comparison with the elastic solution for a cavity in an infinite solid. In this case, irrespective of the form of the spherically symmetrical temperature distribution, Sternberg [10] has shown that the cavity surface displacement remains zero. Because a quasi-static elastic solution depends only on the current geometry and tractions, it follows that $u[a(t),t] = 0$ for the elastic solution corresponding to our ablation problem but with the outer radius b increased to infinity. Substituting this into the expression for $f(t)$ yields the broken curve shown in Fig. 3. It lies close to the finite sphere solution at small times, and the latter gradually falls below it due to the positive radial displacement permitted by the removal of restraint forces at the outer boundary. It is seen that this release is quite small until appreciable ablation has taken place. The reduced peak of circumferential compressive stress in the viscoelastic case reduces the tendency for the outer shell to expand, hence reduces the internal displacement, and so the viscoelastic curve in Fig. 3 lies between the elastic values and that for the infinite elastic sphere.

The stress distributions for the ablating hollow sphere presented here contrast with the solid sphere case described in [6]. In the present case the thermal stress field dies out much less rapidly than for the solid sphere. For the solid sphere the heat from the ablating outer surface heats up the entire sphere and the temperature approaches the uniform value Θ_1. With decreasing temperature gradients, the thermal stresses, even in the elastic case, decrease rapidly with time. The condition of heat transfer across the outer boundary in the present case causes retention of high temperature gradients as is clear from Fig. 2, and this leads to persistence of thermal stresses in both the elastic and viscoelastic cases. Thermal insulation of the outer boundary would reduce these.

As in [6] the dimensions of the sphere (a=4 cms, b=12 cms) and the temperature field (total ablation time 1.4 hrs.) were chosen to illustrate a significant influence of thermo-viscoelasticity. A shorter ablation time would reduce the influence of viscoelasticity for the same temperature range and scale factor $\varphi(T)$. The modest temperature range 80°C to 110°C was chosen for comparison with previous solutions ([5] and [6]), and the effect of temperature on viscoelasticity is so great, that an increase in the upper temperature of the order 100°C could increase φ by several factors of 10, and yield a marked visco-elastic effect even for ablation times of the order of seconds in the same material. Thus quantitative estimates of dominant

relaxation times and the variation of the scale factor $\varphi(T)$ are needed to assess the expected influence of viscoelasticity on a thermal stress problem.

This solution has been presented to illustrate the efficacy of the integral equation approach to a thermo-viscoelastic stress-analysis problem. Numerical solution can be readily processed on an electronic digital computer, and this enables experimentally measured viscoelastic characteristic to be directly introduced into the analysis. This solution goes beyond those previously published in this area, since the analysis reduces to a integral equation spanning both the space and time variables.

$\Delta r/a$ \ $K\Delta t/a^2$		.0125	.025	.05
.05	f(.05)	1.592	1.588	1.604
	f(.1)	2.450	2.442	2.431
	f(.2)	--	4.549	4.519
	f(.4)	--	--	8.350
.10	f(.05)	1.559	1.562	1.593
	f(.1)	2.415	2.412	2.411
	f(.2)	4.580	4.563	4.526
	f(.4)	--	8.369	8.321

Table I. f(t) computed using different time and space steps.

References

1. J. D. Ferry. Structure and mechanical properties of plastics. Die Physik der Hochpolymeren, Ed. by H.A. Stuart, 4, 373-426, 1956.

2. F. Schwarzl and A. J. Staverman. Time-temperature dependence of linear viscoelastic behavior. Jl. Appl. Phys. 23, 838-843, 1952.

3. L. W. Morland and E. H. Lee. Stress analysis for linear viscoelastic materials with temperature variation. Trans. Soc. Rheol. 4, 233-263, 1960.

4. E. H. Lee and T. G. Rogers. Solution of viscoelastic stress analysis problems using measured creep or relaxation functions. To appear in Jl. Appl. Mech. ASME Paper no. 62-WA-18, 1962.

5. R. Muki and E. Sternberg. On transient thermal stresses in viscoelastic materials with temperature-dependent properties. Jl. Appl. Mech. 28, 193-207, 1961.

6. E. H. Lee and T. G. Rogers. Non-linear effects of temperature variation in stress analysis of isothermally linear viscoelastic materials. To appear in the Proceedings of the IUTAM Symposium on Second-Order Effects in Elasticity, Plasticity and Fluid Dynamics, Haifa, 1962.

7. E. Sternberg and M. E. Gurtin. Further study of thermal stresses in viscoelastic materials with temperature-dependent properties. Loc. cit. [6].

8. F. G. Tricomi. Integral equations. Interscience Publishers Inc., New York, 1957.

9. H. S. Carslaw and J. C. Jaeger. Conduction of heat in solids. Clarendon Press, Oxford, p.45, 1947.

10. E. Sternberg. Transient thermal stresses in an infinite medium with a spherical cavity. Proc. Koninkl. Nederl. akad. van Weten., Amsterdam, B60, 396-409, 1957.

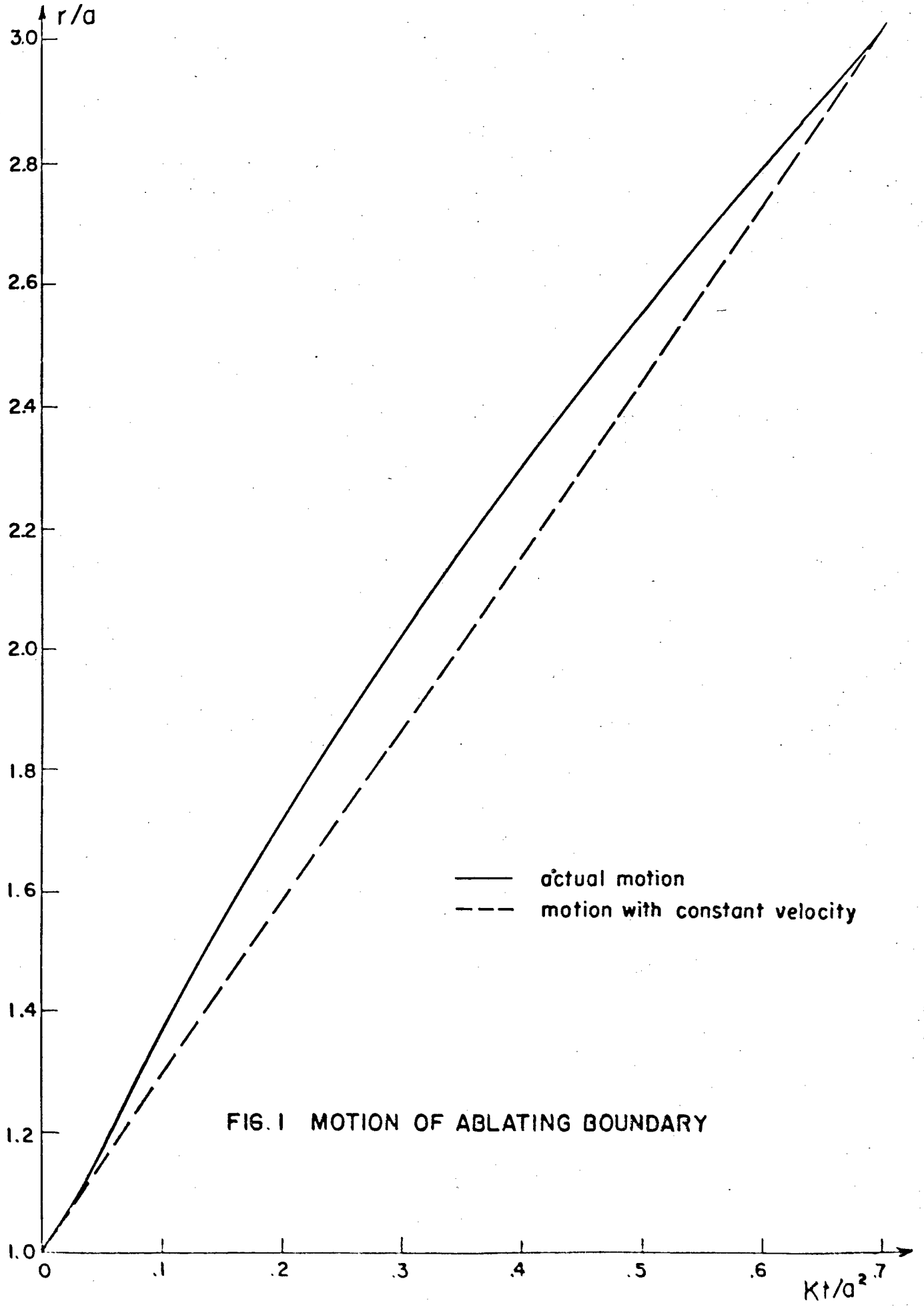

FIG. 1 MOTION OF ABLATING BOUNDARY

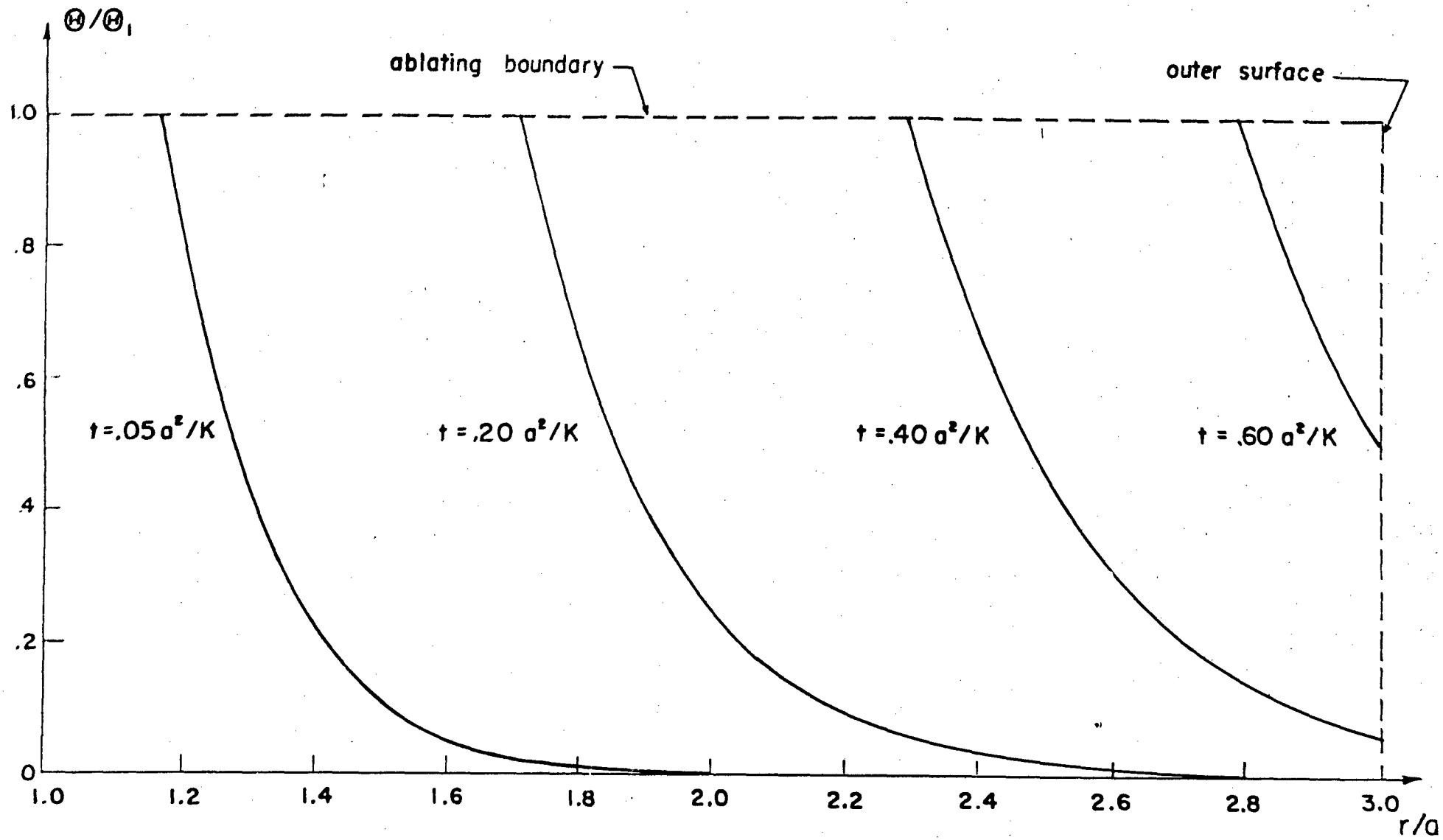

FIG. 2 TEMPERATURE PROFILES AT VARIOUS TIMES

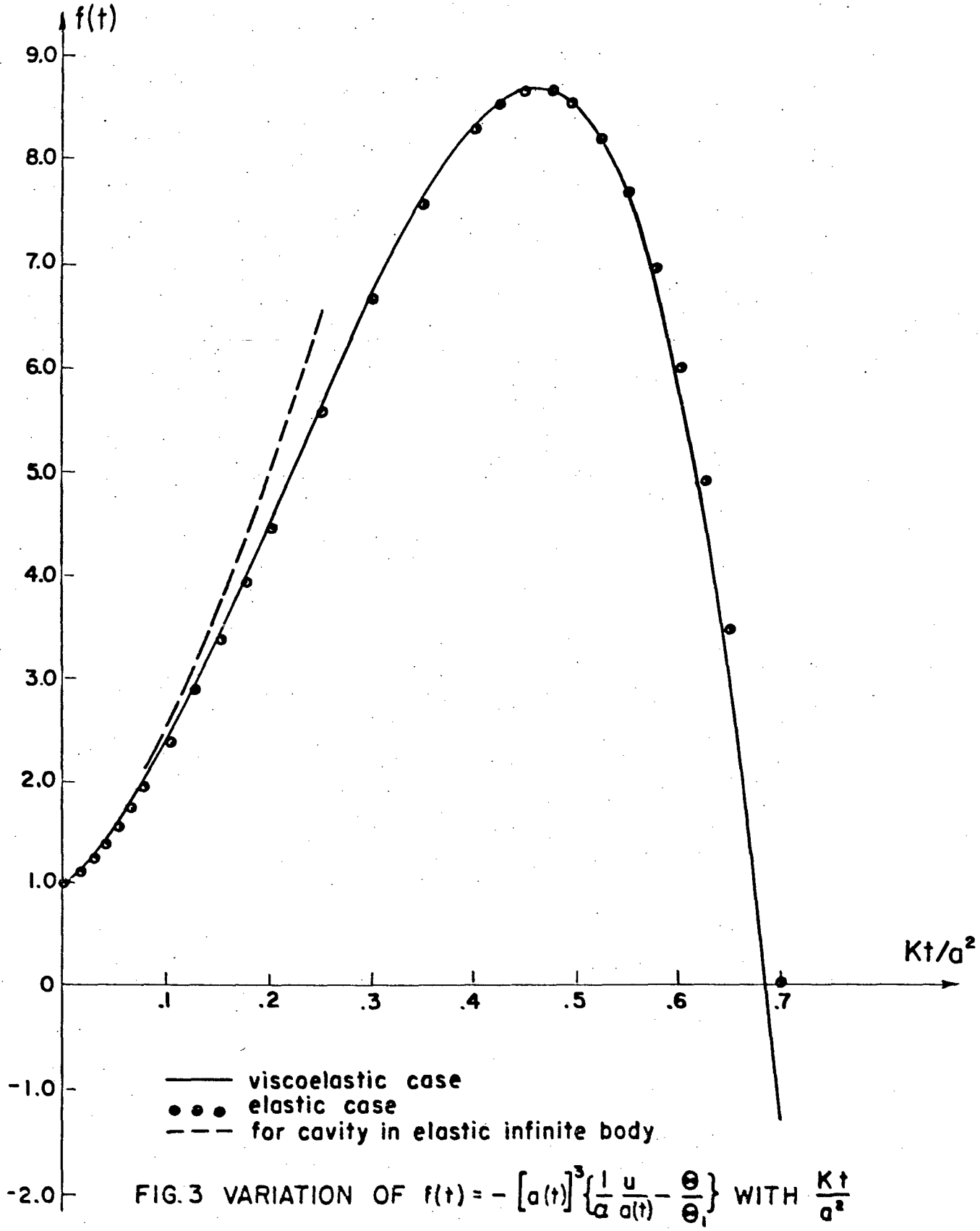

FIG. 3 VARIATION OF $f(t) = -\left[a(t)\right]^3\left\{\frac{1}{\alpha}\frac{u}{a(t)} - \frac{\theta}{\theta_1}\right\}$ WITH $\frac{Kt}{a^2}$

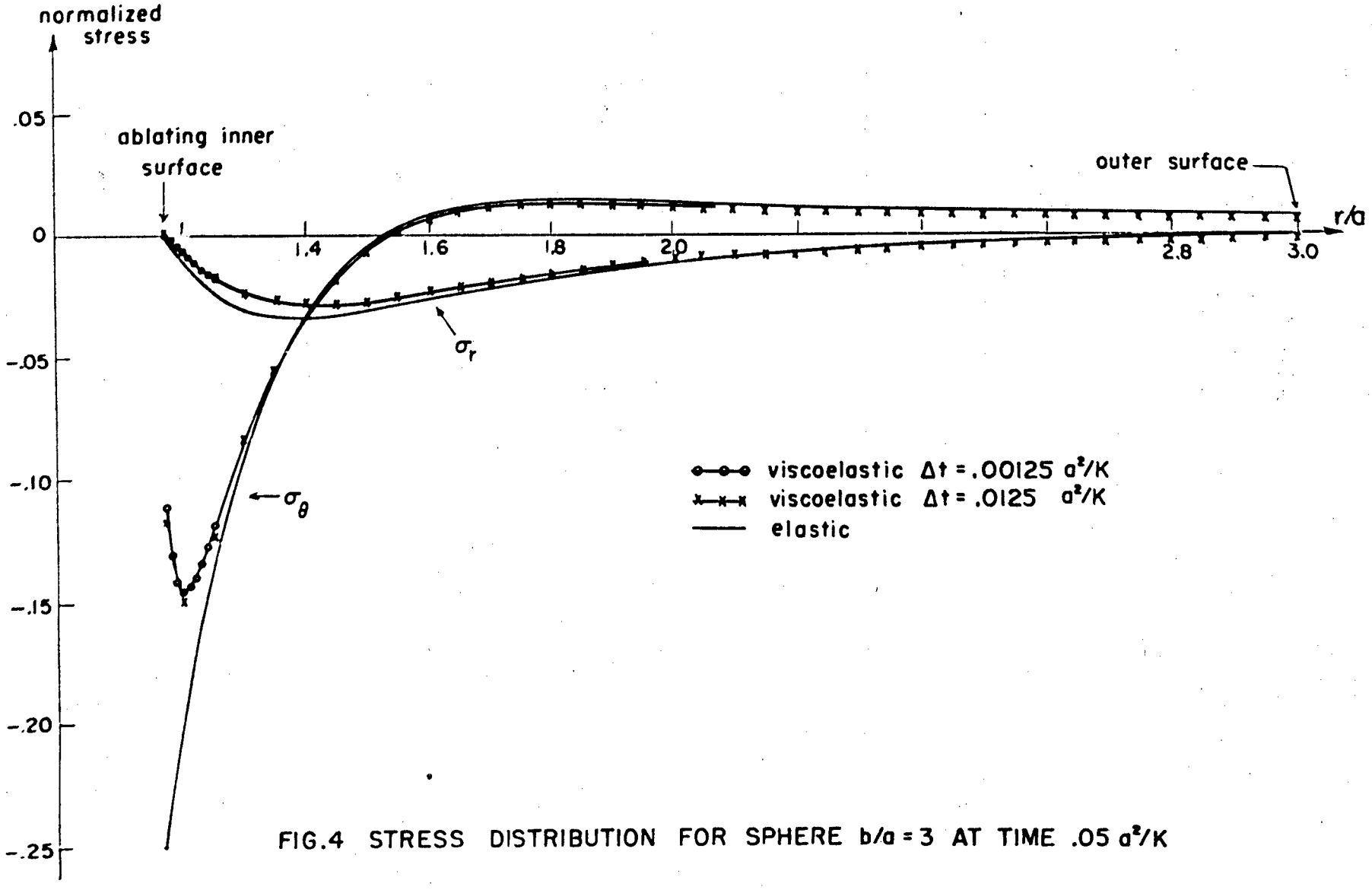

FIG.4 STRESS DISTRIBUTION FOR SPHERE b/a = 3 AT TIME .05 a^2/K

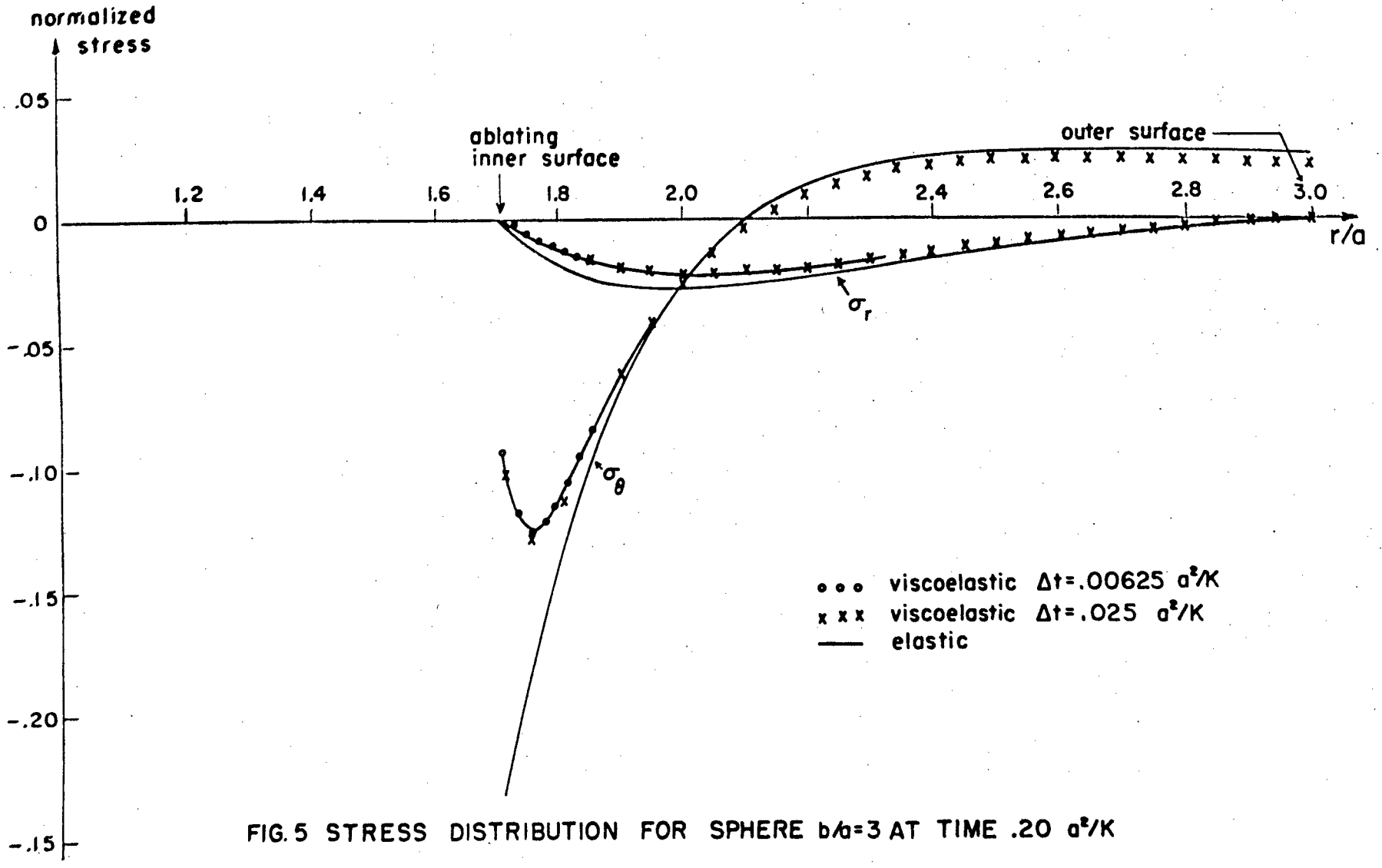

FIG. 5 STRESS DISTRIBUTION FOR SPHERE b/a=3 AT TIME .20 a²/K

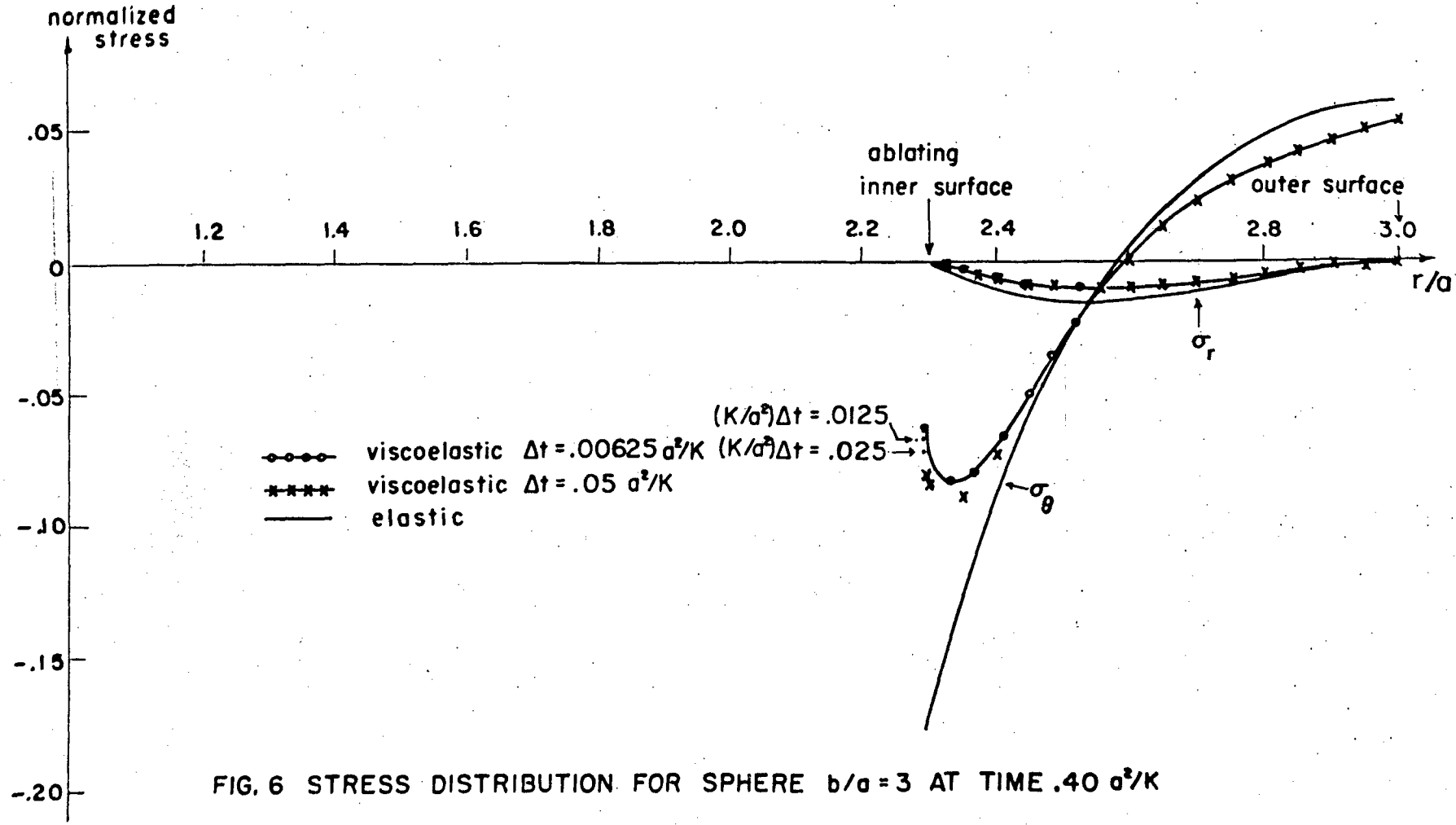

FIG. 6 STRESS DISTRIBUTION FOR SPHERE $b/a = 3$ AT TIME $.40\, a^2/K$

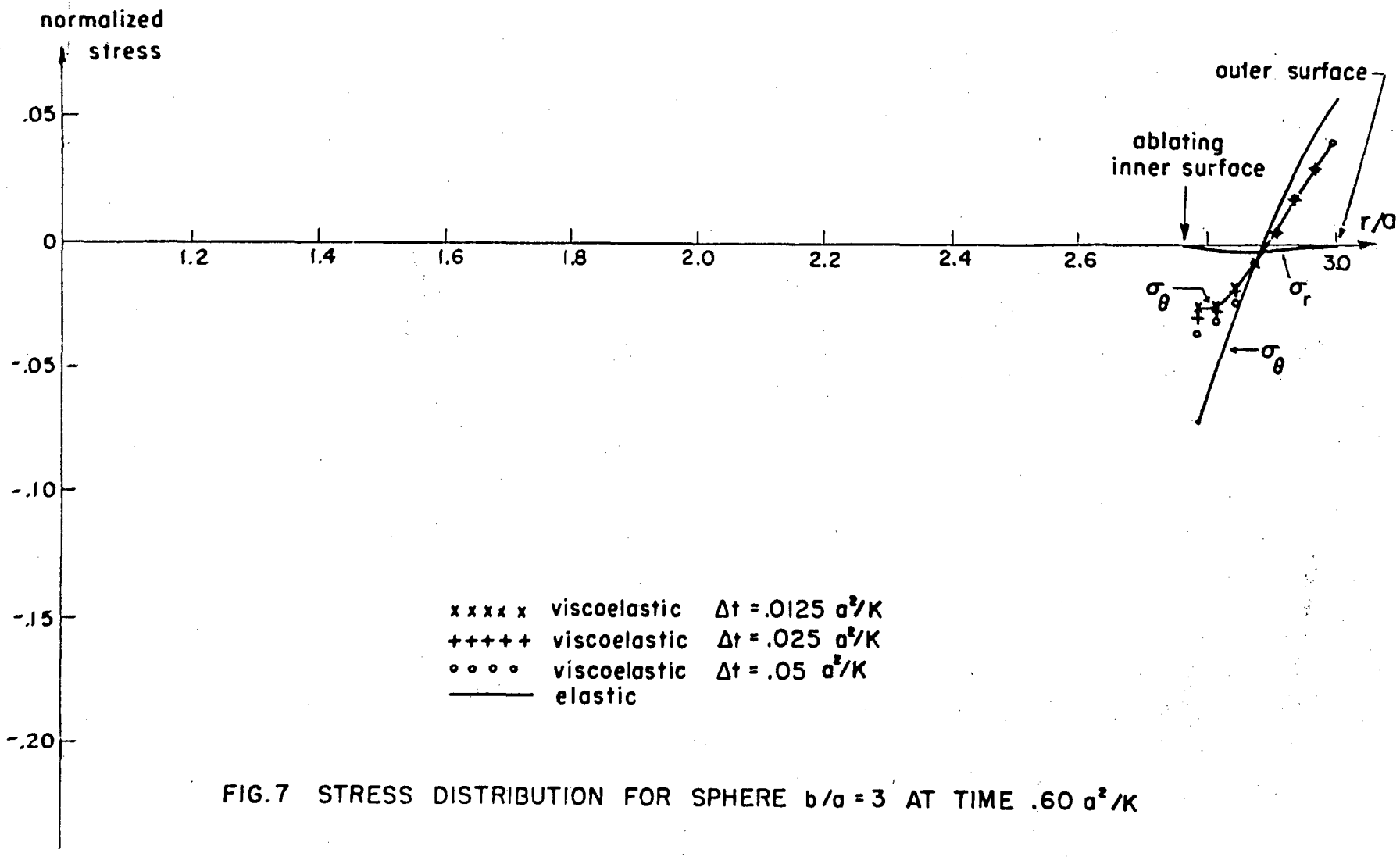

FIG. 7 STRESS DISTRIBUTION FOR SPHERE b/a = 3 AT TIME .60 a^2/K